

## MAJOR PAPER

# Quantification of Endolymphatic Space Volume after Intravenous Administration of a Single Dose of Gadolinium-based Contrast Agent: 3D-real Inversion Recovery versus HYDROPS-Mi2

Toshio Ohashi<sup>1\*</sup>, Shinji Naganawa<sup>2</sup>, Ai Takeuchi<sup>1</sup>, Toshio Katagiri<sup>1</sup>,  
and Kayao Kuno<sup>3</sup>

**Purpose:** Recently, the use of 3D real inversion recovery (3D-real IR) imaging has been proposed for the evaluation of endolymphatic hydrops (EH). This method shows similar contrast between the endolymphatic and perilymphatic spaces and surrounding bone compared with the hybrid of reversed image of positive endolymph signal and native image of perilymph signal multiplied with heavily T<sub>2</sub>-weighted MR cisternography (HYDROPS-Mi2) image. We measured the volume of the endolymphatic space using 3D-real IR and HYDROPS-Mi2 images, and compared the measurements obtained with both techniques.

**Methods:** HYDROPS-Mi2 and 3D-real IR images were obtained for 30 ears from 15 patients with clinical suspicion of EH; imaging was performed 4 h after intravenous administration of a single dose of gadolinium-based contrast agent. We measured the volume of the endolymphatic space in the cochlea and vestibule by manually drawing the regions of interest. The correlation between endolymphatic volume determined from HYDROPS-Mi2 images and 3D-real IR images was calculated.

**Results:** There was a strong positive linear correlation between the cochlear and vestibular endolymphatic volume determined from HYDROPS-Mi2 and 3D-real IR images. The Spearman's rank correlation coefficient ( $\rho$ ) between the measurements obtained with both images was 0.805 ( $P < 0.001$ ) for the cochlea and 0.826 ( $P < 0.001$ ) for the vestibule.

**Conclusion:** The endolymphatic volume measured using 3D-real IR images strongly correlated with that measured using HYDROPS-Mi2 images. Thus, 3D-real IR imaging might be a suitable method for the measurement of endolymphatic volume.

**Keywords:** *endolymphatic hydrops, gadolinium, magnetic resonance imaging, volume quantification*

## Introduction

MR imaging is used for the evaluation of endolymphatic hydrops (EH), a pathological finding associated with Meniere's disease.<sup>1–3</sup> The 3D fluid-attenuated inversion recovery (3D-FLAIR) imaging has high sensitivity to low concentrations

of gadolinium-based contrast agents (GBCAs) in fluid compared with conventional T<sub>1</sub>-weighted imaging.<sup>4</sup> In particular, the heavily T<sub>2</sub>-weighted 3D-FLAIR (hT<sub>2</sub>W-3D-FLAIR) imaging with a long effective echo time is very sensitive to subtle T<sub>1</sub> shortening and can detect low concentration of GBCAs in the perilymphatic space after intravenous administration of a single dose of GBCA (IV-SD-GBCA).<sup>5–7</sup> Furthermore, the subtraction image from two types of hT<sub>2</sub>W-3D-FLAIR imaging with different inversion times after IV-SD-GBCA: hybrid of reversed image of positive endolymph signal and native image of perilymph signal (HYDROPS) technique, and the multiplication image of HYDROPS and MR cisternography (MRC): HYDROPS-multiplied with heavily T<sub>2</sub>-weighted MR cisternography (HYDROPS-Mi2) technique have been proposed to increase the contrast-to-noise ratio (CNR) between the endolymph, perilymph, and bone.<sup>8,9</sup> Separate visualization of the endolymph, perilymph, and bone by

<sup>1</sup>Department of Radiology, Kamiida Daiichi General Hospital, 2-70 Kamiida-kitamachi, Kita-ku, Nagoya, Aichi 462-0802, Japan

<sup>2</sup>Department of Radiology, Nagoya University Graduate School of Medicine, Aichi, Japan

<sup>3</sup>Department of Otorhinolaryngology, Kamiida Daiichi General Hospital, Aichi, Japan

\*Corresponding author, Phone: +81-52-991-3111, Fax: +81-52-981-6879, E-mail: t.ohashi@re.commufa.jp

©2019 Japanese Society for Magnetic Resonance in Medicine

This work is licensed under a Creative Commons Attribution-NonCommercial-NoDerivatives International License.

Received: January 24, 2019 | Accepted: March 27, 2019

these techniques has reduced the difficulty in evaluating EH. Because of this, EH imaging after IV-SD-GBCA has become widely used clinically for the visualization of EH.<sup>2</sup>

The HYDROPS and HYDROPS-Mi2 techniques have the potential risk of misregistration artifacts caused by a patient's movement due to post-image processing for the subtraction or multiplication that is required to generate these images.<sup>8,9</sup> We routinely perform EH imaging 4 h after IV-SD-GBCA using a hT<sub>2</sub>W-3D-FLAIR imaging and quantitatively evaluate the volume of the endolymphatic space using HYDROPS-Mi2 images in accordance with previously reported studies.<sup>9,10</sup> During our repeated evaluation of EH using HYDROPS-Mi2 technique, we have occasionally encountered cases with misregistration artifacts. 3D-real inversion recovery (3D-real IR) imaging, which based on phase-sensitive reconstruction, does not require post processing using multiple imaging to delineate the endolymph and perilymph and can reduce the risk of misregistration artifacts.<sup>11</sup> The conventional 3D-real IR imaging after IV-SD-GBCA has an insufficient CNR to enable separate visualization of the endolymph, perilymph, and surrounding bony structures when evaluating EH. To circumvent these issues, an improved 3D-real IR imaging, which increases the CNR between these structures, was recently proposed.<sup>12</sup> To validate the use of this imaging sequence for the evaluation of EH volume, volume measurements of the endolymphatic space obtained by 3D-real IR imaging should be compared with those obtained by HYDROPS-Mi2 technique.

In this study, we measured the volume of the endolymphatic space using 3D-real IR and HYDROPS-Mi2 images, and compared the measurements obtained by these methods.

## Materials and Methods

### Patients and materials

To assess cases with clinically suspected Meniere's disease, we measured the endolymphatic volume of 30 ears from 15 patients (nine men, six women; ages: 21–70 years, median: 56 years) who underwent MR examination from November, 2017 through September, 2018 and who did not show imaging artifacts caused by the patient's movement. The estimated glomerular filtration rate of all patients exceeded 60 mL/min/1.73 m<sup>2</sup>. The medical ethics committee of our hospital approved this retrospective study and waived informed consent. All MR scans used in this study were performed on a 3T MR scanner (MAGNETOM Skyra; Siemens Healthcare, Erlangen, Germany) with a 32-channel phased-array head coil, and images were obtained 4 h after IV-SD-GBCA. The GBCA administered to patients in this study was a macrocyclic GBCA (Gd-HP-DO3A: ProHance, Eisai, Tokyo, Japan). A single dose of GBCA was defined as 0.1 mmol/kg body weight. A DICOM viewer (OsiriX version 5.8 32 bit; Pixmeo SARL, Bernex, Switzerland, <http://www.osirix-viewer.com/>) was used for image processing and analysis. Statistical analyses were performed with software R (version 3.4.3, The R Foundation for Statistical Computing, Vienna, Austria, <https://www.R-project.org/>).

### MR imaging

All imaging sequences were based on a hT<sub>2</sub>W 3D-turbo spin echo (TSE) imaging with a variable refocusing flip angle. We obtained four types of images: MRC, positive perilymph image (PPI), positive endolymph image (PEI), and 3D-real IR image. The details of the sequence parameters are listed in Table 1. For MRC imaging, an hT<sub>2</sub>W-3D-TSE imaging (TR = 4400 ms, TE = 544 ms) without an IR pulse was applied. For imaging of PPI or PEI, an hT<sub>2</sub>W-3D-TSE imaging with TR (9000 ms) and a nonselective IR pulse (PPI: 2250 ms, PEI: 2050 ms) to suppress the endolymphatic or perilymphatic space signals was applied. For 3D-real IR imaging, an hT<sub>2</sub>W-3D-TSE imaging, which had been reconstructed phase-sensitively, with an extended TR (15,130 ms) and a nonselective IR pulse (2700 ms) to suppress the endolymphatic space signal was applied. The oblique degree of the slab for all sequences was parallel to the anterior commissure (AC)–posterior commissure (PC) line and bilateral internal auditory canal in the axial plane. The slab thickness for MRC, PPI, and PEI was 104 mm, and the slab center was set at the level of the internal auditory canal. The slab thickness for 3D-real IR imaging was 256 mm, and the slab center was set at the level of the mammillary body. The voxel size of all sequences was 0.5 × 0.5 × 1.0 mm. The HYDROPS-Mi2 images were generated according to the following methods which were described in a previous study.<sup>9</sup>

$$\text{HYDROPS} = \text{PPI} - \text{PEI}$$

$$\text{HYDROPS-Mi2} = \text{HYDROPS} \times \text{MRC}$$

We confirmed that there were no misregistration artifacts greater than 1 mm in any patient for the HYDROPS-Mi2 images.

### Image analysis

We corrected the slight position gap between the MRC, HYDROPS-Mi2, and 3D-real IR images using the position correction program of OsiriX by manually designating pixels. Two radiographers with 15 (T.O.) and 7 years (A.T.) of experience in MR imaging manually drew the ROIs along the boundary of the cochlea and the vestibule on all MRC slices according to previously reported methods.<sup>10</sup> The ROIs from the MRC images were copied and pasted onto the HYDROPS-Mi2 and the 3D-real IR images. An example of the ROI segmentation is shown in Fig. 1. In this study, we regarded all voxels within the ROIs as representing the total lymphatic space, and the voxels within the ROIs indicating negative signal intensity were defined as the endolymphatic space. The number of voxels representing the total lymphatic and the endolymphatic spaces were counted for all image slices from the HYDROPS-Mi2 and the 3D-real IR. The percentage of the volume of the endolymphatic space in the total lymphatic space (%EL<sub>volume</sub>) was defined as follows:<sup>10</sup>

$$\%EL_{\text{volume}} = (\text{sum of the number of negative voxels representing the endolymph in the ROIs from all slices divided by the total number of voxels in the ROIs of all slices}) \times 100.$$

**Table 1** Pulse sequence parameters

Parameter	MRC	PPI and PEI	3D-real IR
Sequence type	SPACE with restore pulse	SPACE with inversion pulse	SPACE with inversion pulse
Repetition time (ms)	4400	9000	15,130
Echo time (ms)	544	544	549
Inversion time (ms)	NA	PPI: 2250/PEI: 2050	2700
Fat suppression	CHESS	CHESS	CHESS
Flip angle (°)	90/initial 180 decrease to constant 120	90/constant 180	90/constant 180
Section thickness/gap (mm)	1.0/0.0	1.0/0.0	1.0/0.0
Pixel size (mm)	0.5 × 0.5	0.5 × 0.5	0.5 × 0.5
Number of slices	104	104	256
Echo train length	173	173	256
Field of view (mm)	165 × 196	165 × 196	165 × 196
Matrix size	324 × 384	324 × 384	324 × 384
Parallel imaging/Accel. factor	GRAPPA/2	GRAPPA/2	GRAPPA/3
Band width (Hz/Px)	434	434	434
Excitation	Slab selective	Slab selective	Non-slab selective
Number of excitations	1.8	2	1
Scan time (min)	3.4	7.4	11.4

CHESS, chemical shift selective; GRAPPA, generalized auto-calibrating partially parallel acquisition; MRC, magnetic resonance cisternography; NA, not applicable; PEI, positive endolymph image; PPI, positive perilymph image; SPACE, sampling perfection with application-optimized contrasts using different flip angle evolutions; 3D-real IR, 3D real inversion recovery with phase sensitive reconstruction.

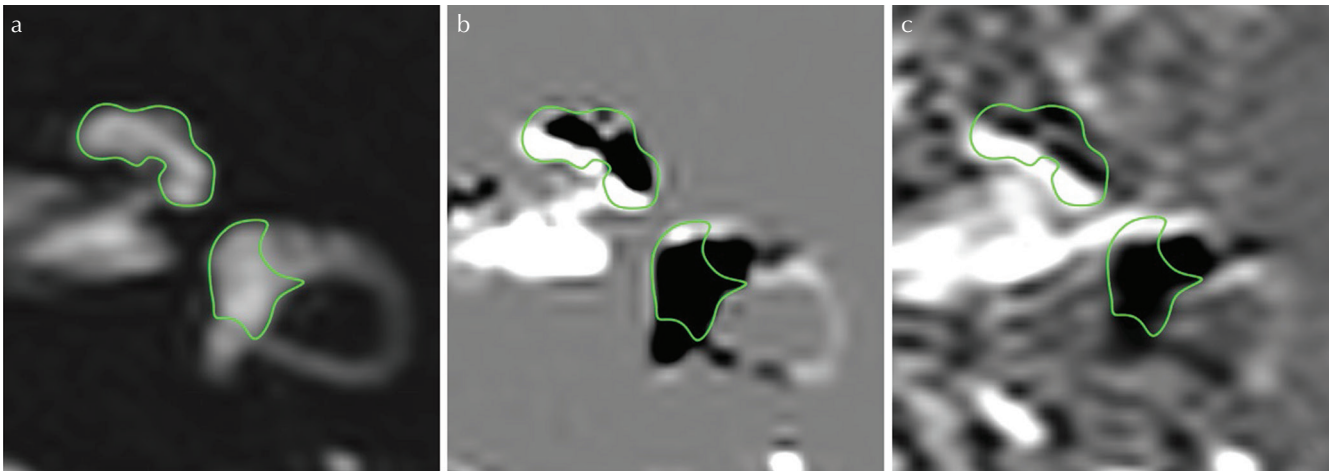


**Fig. 1** An example of a ROI for the measurement of endolymphatic volume. The ROIs were manually drawn along the boundary of the cochlea and vestibule using magnetic resonance cisternography (MRC) (a). The ROIs were copied and pasted onto the hybrid of reversed image of positive endolymph signal and the native perilymph image using the signal-multiplied with heavily T<sub>2</sub>-weighted MR cisternography (HYDROPS-Mi2) image (b) and the 3D-real inversion recovery (3D-real IR) image (c).

The cochlear and the vestibular %EL<sub>volume</sub> from the HYDROPS-Mi2 and 3D-real IR images were calculated.

The intra-class correlation coefficients (ICCs) between the measurements obtained by the two observers were calculated. The correlation between the %EL<sub>volume</sub> from the HYDROPS-Mi2 images and the 3D-real IR images was evaluated by a Spearman's rank correlation coefficient

using the mean value of the two observers' measurements. The significant difference between the %EL<sub>volume</sub> from the HYDROPS-Mi2 images and the 3D-real IR images was evaluated by the Wilcoxon signed-rank test using the mean value of the two observers' measurements. We considered a probability value <0.05 as statistically significant.

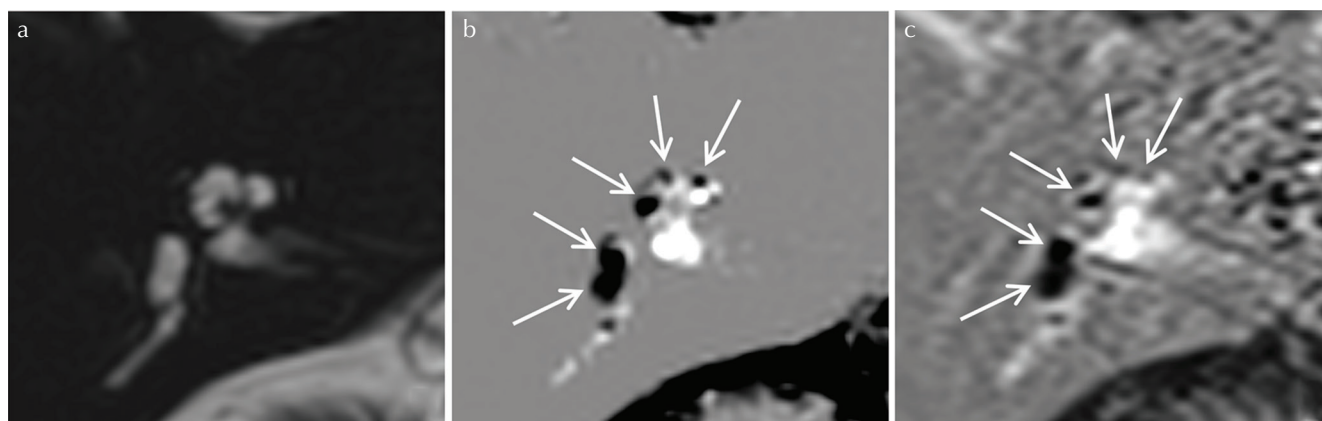


**Fig. 2** Representative images. A 55-year-old woman with significant endolymphatic hydrops (EH); magnetic resonance cysternography (MRC) (a); hybrid of reversed image of positive endolymph signal and native image of the perilymph signal-multiplied with heavily  $T_2$ -weighted MR cysternography (HYDROPS-Mi2) image (b); 3D-real inversion recovery (3D-real IR) image (c). The EH is clearly visible in the HYDROPS-Mi2 and 3D-real IR images (arrows).

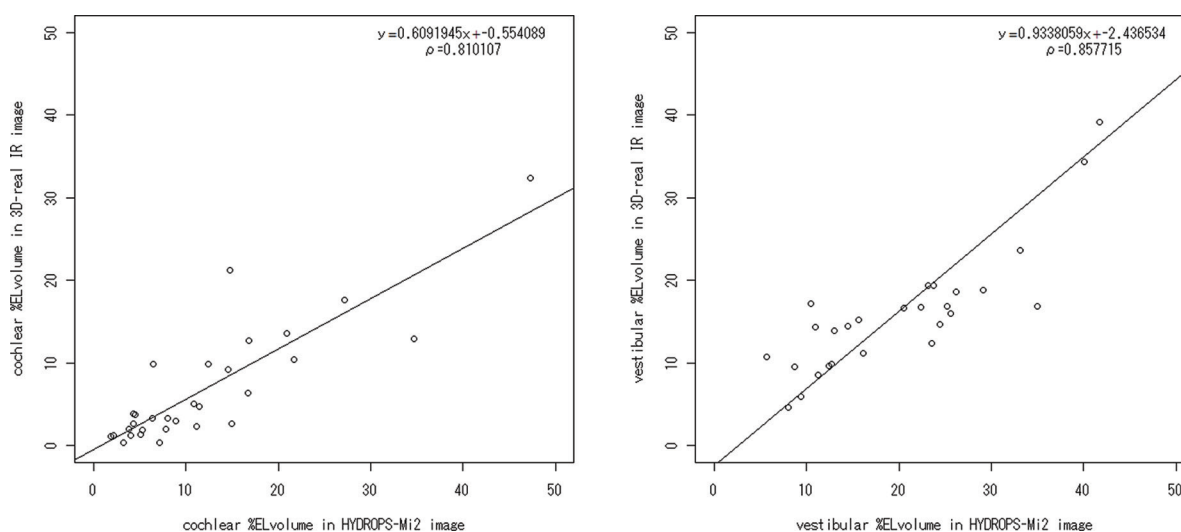


**Fig. 3** Scatterplots of the  $\%EL_{\text{volume}}$  showing the correlation between the HYDROPS-Mi2 images and 3D-real IR images. There is a strong positive linear correlation between the  $\%EL_{\text{volume}}$  of the cochlea and vestibule from the HYDROPS-Mi2 images and the 3D-real IR images. The Spearman's rank correlation coefficient ( $\rho$ ) between the  $\%EL_{\text{volume}}$  of the HYDROPS-Mi2 images and the 3D-real IR images is 0.805 ( $P < 0.001$ ) for the cochlea and 0.826 ( $P < 0.001$ ) for the vestibule. HYDROPS-Mi2, hybrid of reversed image of positive endolymph signal and native image of perilymph signal-multiplied with heavily  $T_2$ -weighted magnetic resonance imaging cysternography; 3D-real IR, 3D-real inversion recovery;  $\%EL_{\text{volume}}$ , the percentage of the volume of the endolymphatic space in the total lymphatic space.

## Results

Representative images obtained in this study are shown in Fig. 2. The ICCs between the measurements of the two observers were 0.982 for the cochlear  $\%EL_{\text{volume}}$  and 0.989 for the vestibular  $\%EL_{\text{volume}}$ . There was a strong positive linear correlation between the cochlear and vestibular  $\%EL_{\text{volume}}$  of the HYDROPS-Mi2 images and the 3D-real IR images (Fig. 3). The Spearman's rank correlation coefficient ( $\rho$ ) between the  $\%EL_{\text{volume}}$  of the HYDROPS-Mi2 images and the 3D-real IR images was 0.805 ( $P < 0.001$ ) for the cochlea and 0.826 ( $P < 0.001$ ) for the vestibule. The cochlear and vestibular median  $\%EL_{\text{volume}}$  of the 3D-real IR images

was significantly lower value than that of the HYDROPS-Mi2 images ( $P < 0.001$ ).

## Discussion

In this study, there was a strong positive linear correlation between the HYDROPS-Mi2 and the 3D-real IR images for both the cochlear and vestibular endolymphatic volume measurements, and the cochlear and vestibular endolymphatic volume of the 3D-real IR images was significantly lower value than that of the HYDROPS-Mi2 images. Judging from the slope of the graphs (Fig. 3a and 3b), the endolymphatic volume obtained using 3D-real IR images tends to show a lower

value compared to the HYDROPS-Mi2 images especially in the cochlear measurement.

Although the utricle and the saccule, which contain the vestibular endolymph, are oblong-shaped organs of reasonable size, the cochlear duct containing the cochlear endolymph is a ductal organ of smaller size. Due to the morphological differences in these structures, the cochlear endolymph tends to appear as a smaller structure than the vestibular endolymph in axial sections from MR imaging. The number of pixels representing the cochlear endolymph on a single MR image was typically 5–9 pixels even in cases diagnosed as having “significant endolymphatic hydrops” using the Nakashima grade. The ratio of the pixels located on a boundary between the endolymph and perilymph to the pixels of the endolymphatic space is larger in the cochlea compared with the vestibule.

The HYDROPS-Mi2 technique provides a sufficient CNR to accurately divide the cochlear endolymphatic and perilymphatic spaces, as the individual signals of the endolymph, perilymph and the total lymphatic space are obtained separately and these images are arithmetically processed to generate the HYDROPS-Mi2 image.<sup>9</sup> With the 3D-real IR imaging the endolymph and perilymph signals are obtained in a single acquisition; it also has a longer echo train length that causes more blurring artifacts compared with PPI and PEI. Therefore, the evaluation of the endolymphatic space in the cochlea is more sensitive to the partial volume effect compared with that in the vestibule, especially on 3D-real IR images. This characteristic of 3D-real IR images should be considered when applying 3D-real IR imaging to the quantification of EH volume ratio in the cochlea.

The acquisition time for 3D-real IR images is shorter (11 min) than for HYDROPS-Mi2 images (18 min); moreover, the 3D-real IR imaging does not require post-imaging processing. The results of this study suggest that the 3D-real IR imaging is a potential alternative method to the HYDROPS-Mi2 technique for quantification of the endolymphatic space. Further study is warranted to improve the CNR of the 3D-real IR images between the endolymph and perilymph for clear quantification of the endolymphatic space.

Subjective evaluation methods such as the saccule-to-utricle ratio inversion (SURI)<sup>13</sup> and the presence of the vestibular endolymphatic space contacting the oval window (VESCO)<sup>14</sup> have been utilized in conjunction with 3D-FLAIR images. However, the presence of EH was only evaluated using 3D-FLAIR images after IV-GBCA in these studies.<sup>13,14</sup> Using only 3D-FLAIR images, it is not possible to differentiate between bone, air, and the endolymphatic space. Even for these subjective evaluation methods, it might be easier to use 3D-real IR imaging than to use 3D-FLAIR imaging. Furthermore, the study evaluating the VESCO<sup>14</sup> utilized a double dose of IV-GBCA. With our method utilizing the 3D-real IR imaging we can evaluate the SURI and the VESCO, as well as the volume of the endolymphatic space in cochlea and vestibule, respectively, after only a single dose of IV-GBCA.

## Limitations

This study has a few limitations. We evaluated only a small number of patients. The placement of the ROI was performed manually, although measurements from two observers indicated good agreement. The order of the image acquisition was not randomized, although the time lag between each scan did not affect the size of the EH in regards to the time course of the perilymph enhancement.<sup>15</sup> The true value of the endolymphatic volume was unknown, although the EH volume ratio by the HYDROPS-Mi2 and the 3D-real IR images showed strong correlation.

## Conclusion

The endolymphatic volume measured using 3D-real IR images strongly correlated to that measured using HYDROPS-Mi2 images. Thus, 3D-real IR imaging might be suitable as a substitute sequence for HYDROPS-Mi2 imaging.

## Conflicts of Interest

None of the authors have any conflicts of interest regarding this study.

## References

1. Nakashima T, Naganawa S, Pyykko I, et al. Grading of endolymphatic hydrops using magnetic resonance imaging. *Acta Otolaryngol Suppl* 2009; 129:5–8.
2. Naganawa S, Nakashima T. Visualization of endolymphatic hydrops with MR imaging in patients with Ménière’s disease and related pathologies: current status of its methods and clinical significance. *Jpn J Radiol* 2014; 32:191–204.
3. Nakashima T, Pyykko I, Arroll MA, et al. Meniere’s disease. *Nat Rev Dis Primers* 2016; 2:16028.
4. Fukuoka H, Hirai T, Okuda T, et al. Comparison of the added value of contrast-enhanced 3D fluid-attenuated inversion recovery and magnetization-prepared rapid acquisition of gradient echo sequences in relation to conventional postcontrast T<sub>1</sub>-weighted images for the evaluation of leptomeningeal diseases at 3T. *AJNR Am J Neuroradiol* 2010; 31:868–873.
5. Naganawa S, Kawai H, Sone M, Nakashima T. Increased sensitivity to low concentration gadolinium contrast by optimized heavily T<sub>2</sub>-weighted 3D-FLAIR to visualize endolymphatic space. *Magn Reson Med Sci* 2010; 9: 73–80.
6. Naganawa S. The technical and clinical features of 3D-FLAIR in neuroimaging. *Magn Reson Med Sci* 2015; 14:93–106.
7. Naganawa S, Yamazaki M, Kawai H, Bokura K, Sone M, Nakashima T. Visualization of endolymphatic hydrops in Ménière’s disease with single-dose intravenous gadolinium-based contrast media using heavily T<sub>2</sub>-weighted 3D-FLAIR. *Magn Reson Med Sci* 2010; 9:237–242.
8. Naganawa S, Yamazaki M, Kawai H, Bokura K, Sone M, Nakashima T. Imaging of Ménière’s disease after

- intravenous administration of single-dose gadodiamide: utility of subtraction images with different inversion time. *Magn Reson Med Sci* 2012; 11:213–219.
9. Naganawa S, Suzuki K, Nakamichi R, et al. Semi-quantification of endolymphatic size on MR imaging after intravenous injection of single-dose gadodiamide: comparison between two types of processing strategies. *Magn Reson Med Sci* 2013; 12:261–269.
  10. Naganawa S, Ohashi T, Kanou M, Kuno K, Sone M, Ikeda M. Volume quantification of endolymph after intravenous administration of a single dose of gadolinium contrast agent: comparison of 18- versus 8-minute imaging protocols. *Magn Reson Med Sci* 2015; 14: 257–262.
  11. Naganawa S, Satake H, Kawamura M, Fukatsu H, Sone M, Nakashima T. Separate visualization of endolymphatic space, perilymphatic space and bone by a single pulse sequence; 3D-inversion recovery imaging utilizing real reconstruction after intratympanic Gd-DTPA administration at 3 Tesla. *Eur Radiol* 2008; 18:920–924.
  12. Naganawa S, Kawai H, Taoka T, Sone M. Improved 3D-real inversion recovery: a robust imaging technique for endolymphatic hydrops after intravenous administration of gadolinium. *Magn Reson Med Sci* 2019; 18:105–108.
  13. Attyé A, Eliezer M, Boudiaf N, et al. MRI of endolymphatic hydrops in patients with Meniere’s disease: a case-controlled study with a simplified classification based on saccular morphology. *Eur Radiol* 2017; 27:3138–3146.
  14. Conte G, Caschera L, Calloni S, et al. MR imaging in Menière disease: is the contact between the vestibular endolymphatic space and the oval window a reliable biomarker? *AJNR Am J Neuroradiol* 2018; 39:2114–2119.
  15. Naganawa S, Suzuki K, Yamazaki M, Sakurai Y, Ikeda M. Time course for measuring endolymphatic size in healthy volunteers following intravenous administration of gadoteridol. *Magn Reson Med Sci* 2014; 13:73–80.